SUPPLEMENTARY APPENDIX

Impaired cytotoxicity associated with defective natural killer cell differentiation in myelodysplastic syndromes

Maryam Hejazi,[1] Angela R. Manser,[1] Julia Fröbel,[2] Andrea Kündgen,[2] Xiaoyi Zhao,[1] Kathrin Schönberg,[1] Ulrich Germing,[2] Rainer Haas,[2] Norbert Gattermann,[2] and Markus Uhrberg[1]

[1]Institute for Transplantation Diagnostics and Cell Therapeutics, Medical Faculty, Heinrich-Heine University Düsseldorf; and [2]Department of Hematology, Oncology and Clinical Immunology, Medical Faculty, Heinrich-Heine University Düsseldorf, Germany

 doi:10.3324/haematol.2014.118679
Manuscript received on October 13, 2014. Manuscript accepted on February 9, 2015.
Correspondence: Markus.Uhrberg@med.uni-duesseldorf.de

Supplementary methods

Cell lines

The HLA class I-deficient target cell line K562 was grown in DMEM (Gibco, CA, USA) supplemented with 10% FBS and 1% Penicillin/Streptomycin/L-Glutamine (Gibco).

Annexin V apoptosis assay

Apoptosis of NK cells in MDS patients and healthy age-matched donors was determined using the Annexin V detection Kit (Biolegend). Briefly, PBMCs were stained with fluorescence-labeled CD56 and CD3 surface marker. After washing with PBS, Annexin V-FITC and 7-AAD was added. Apoptotic NK cells were identified as Annexin V^+ 7-AAD^- NK cells by flow cytometry.

KIR genotyping

Genomic DNA was isolated from blood of MDS patients and healthy age-matched donors via QiaAmp DNA Blood Mini Kit (Qiagen). KIR genotyping was performed by polymerase chain reaction with sequence specific primer (PCR-SSP) as reported previously.[1]

NK cell stimulation

$1x10^5$ CD3-depleted PBMC (CD3 Microbeads, Miltenyi Biotech) were incubated in a 24-well tissue culture plate with $1x10^5$ irradiated K562 and $1x10^6$ irradiated feeder PBMC (pooled from 3 different donors) with 1000 U/ml IL-2 in RPMI 1640, 10% FBS and 5% human serum type AB. Medium was exchanged every two days with fresh medium.

1. Vilches C, Castano J, Gomez-Lozano N, Estefania E. Facilitation of KIR genotyping by a PCR-SSP method that amplifies short DNA fragments. *Tissue Antigens.* 2007;70(5):415-422

.

Supplementary figure legends:

Figure S1: Decreased frequency of NK cells in MDS patients. Frequency of NK cells ($CD56^+CD3^-$) in healthy adult donors (n=116; age 18-50) compared to MDS patients (n=75). Statistical significance was determined by two-tailed *t*-test (***p<0.001).

Figure S2: Correlation between frequency of NK cells and cytotoxicity in MDS patients. Specific lysis of K562 is plotted versus frequency of NK cells among PBMC of MDS patients (linear regression analysis, p=0.136).

Figure S3: Reduced IFN-ɣ production in MDS patients. Intracellular IFN-ɣ production by IL-2-stimulated NK cells after co-culture with K562 in patients (n=10) and healthy age-matched donors (n=7). Statistical significance was determined by two-tailed *t*-test (*p<0.05).

Figure S4: Association between cytotoxicity and levels of granzyme B and perforin in MDS patients. NK cells of 5 MDS patients and one healthy age-matched donor were enriched to 80-90% purity (EasySep™ Human NK Cell Enrichment Kit, Stemcell Technologies). Cytotoxicity as well as intracellular staining of granzyme B and perforin were performed as described in the Methods section. Filled dots represent patients with low NK cell function (specific lysis of K562 <20%) and open dots patients with normal NK cell function (specific lysis of K562 ≥20%). The open triangle represents a healthy age-matched controls with normal NK cell function. (linear regression analysis, p=0.0019).

Figure S5: Annexin V-determined apoptosis of $CD56^{dim}$ and $CD56^{bright}$ NK cell. PBMC of MDS patients (n=20) and healthy age-matched donors (n=13) were thawed. Annexin V apoptosis assay was performed and the frequency of

apoptotic cells (Annexin V^+7-AAD^-) was determined in the $CD56^{dim}$ (A) and $CD56^{bright}$ NK cell (B). (C) Correlation between frequency of apoptotic NK cells and absolute number of NK cells in MDS patients (linear regression analysis, p=0.585).

Figure S6: KIR repertoires in MDS patients and healthy age-matched donors according to presence of group A and B haplotypes. Frequency of 16 KIR (KIR2DL1, KIR2DL2/3 and KIR3DL1) and NKG2A receptor combinations, ordered according to number of expressed receptors in MDS patients (A/A: n=10, B/x: n=20) and healthy age-matched donors (A/A: n=6, B/x: n=14) with A/A haplotype (A) and B/x haplotype (B). Statistical significance was determined by two-tailed *t*-test (*p<0.05, **p<0.01).

Figure S7: Increased expression of CD62L on NK cells in MDS. Surface expression of CD57, CD62L, NKG2D, NKp30 and CD16 on NK cells of MDS patients (n=16) and healthy age-matched donors (n=10). Statistical significance was determined by two-tailed *t*-test (*p<0.05).

Figure S8: Expression of CD16 on $CD56^{dim}$ and $CD56^{bright}$ NK cells. Frequency of CD16 on $CD56^{dim}$ and $CD56^{bright}$ NK cells of 15 MDS patients and 5 healthy age-matched controls. Statistical significance was determined by two-tailed *t*-test (*p<0.05).

Figure S9: Reduced granzyme B and perforin content in $CD107^+$ NK cells of MDS patients. Box plots showing frequencies of granzyme B (A) and perforin (B) expressing NK cells when restricting analysis to the $CD107^+$ subset. Intracellular granzyme B and perforin were analyzed in $CD56^+CD107^+$ cells following stimulation with K562. Statistical significance was determined by two-tailed *t*-test (*p<0.05, **p<0.01, ***p<0.001).

Supplementary figures:

Figure S1

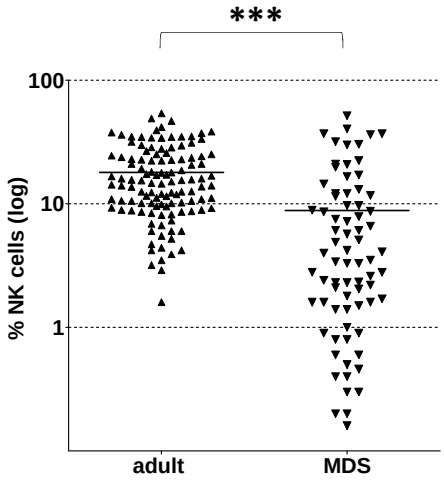

Figure S2

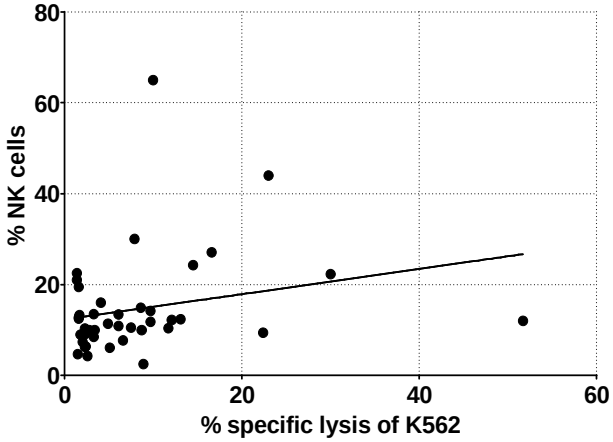

Figure S3

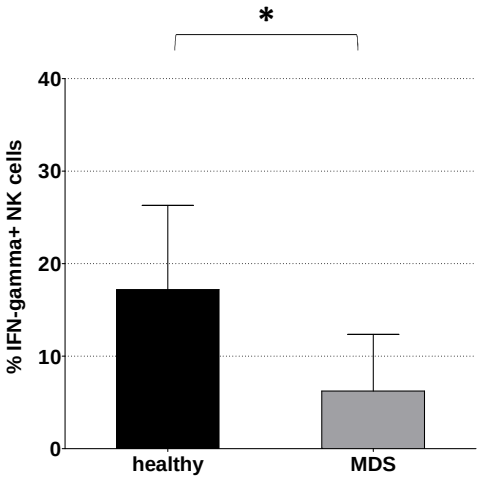

Figure S4

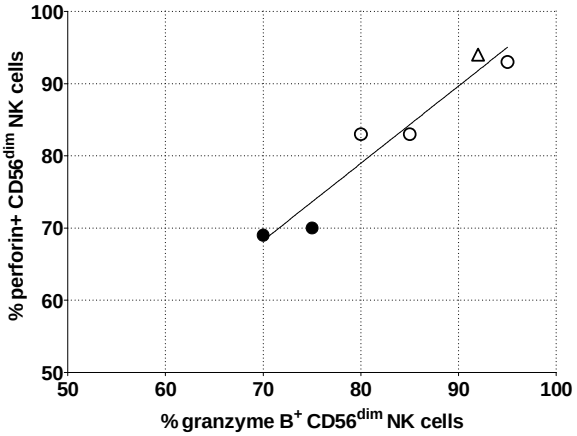

Figure S5

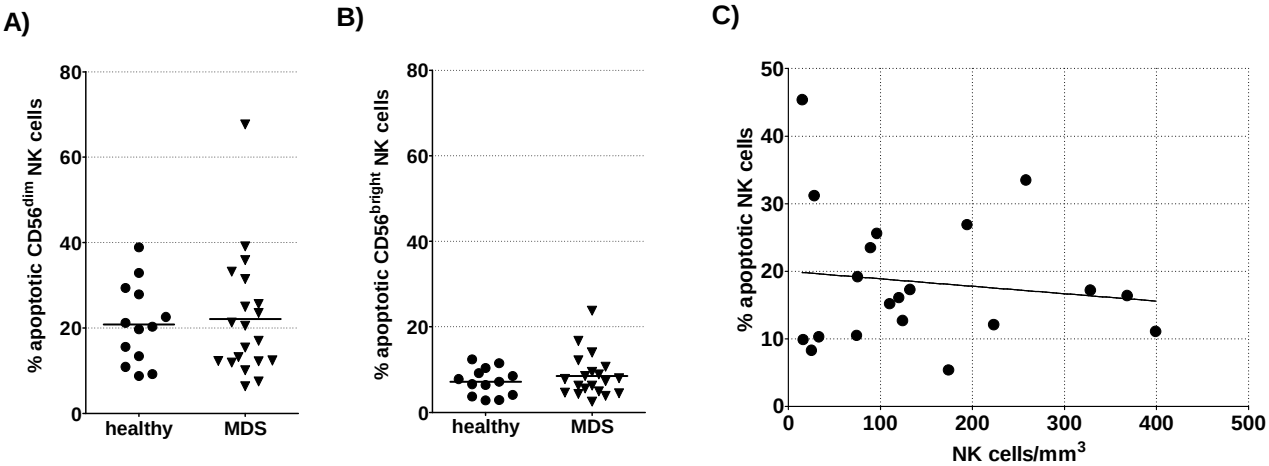

Figure S6

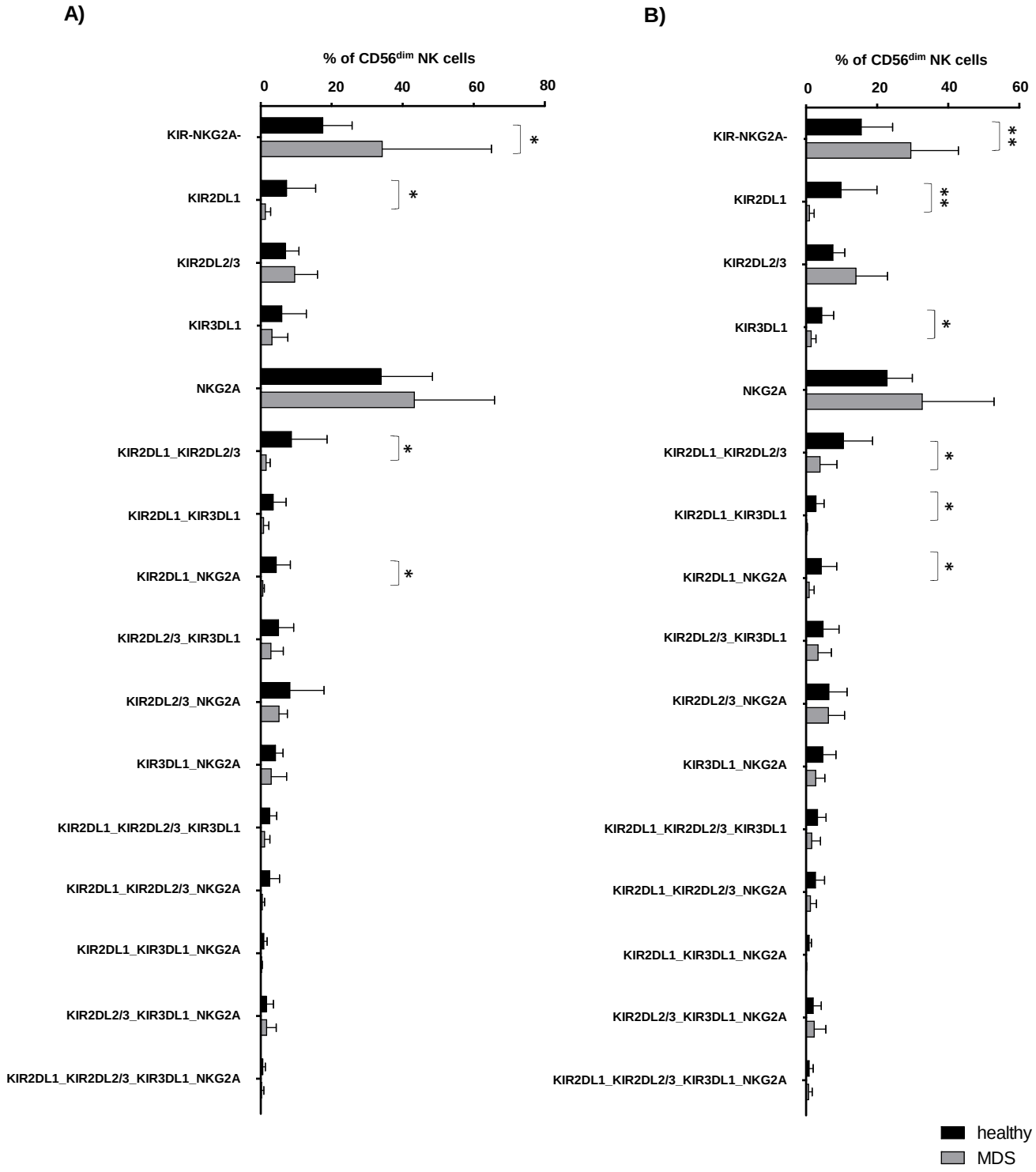
A)
% of CD56dim NK cells
0
20
40
60
80
KIR-NKG2A-
KIR2DL1
KIR2DL2/3
KIR3DL1
NKG2A
KIR2DL1_KIR2DL2/3
KIR2DL1_KIR3DL1
KIR2DL1_NKG2A
KIR2DL2/3_KIR3DL1
KIR2DL2/3_NKG2A
KIR3DL1_NKG2A
KIR2DL1_KIR2DL2/3_KIR3DL1
KIR2DL1_KIR2DL2/3_NKG2A
KIR2DL1_KIR3DL1_NKG2A
KIR2DL2/3_KIR3DL1_NKG2A
KIR2DL1_KIR2DL2/3_KIR3DL1_NKG2A
B)
% of CD56dim NK cells
0
20
40
60
KIR-NKG2A-
KIR2DL1
KIR2DL2/3
KIR3DL1
NKG2A
KIR2DL1_KIR2DL2/3
KIR2DL1_KIR3DL1
KIR2DL1_NKG2A
KIR2DL2/3_KIR3DL1
KIR2DL2/3_NKG2A
KIR3DL1_NKG2A
KIR2DL1_KIR2DL2/3_KIR3DL1
KIR2DL1_KIR2DL2/3_NKG2A
KIR2DL1_KIR3DL1_NKG2A
KIR2DL2/3_KIR3DL1_NKG2A
KIR2DL1_KIR2DL2/3_KIR3DL1_NKG2A
healthy
MDS

Figure S7

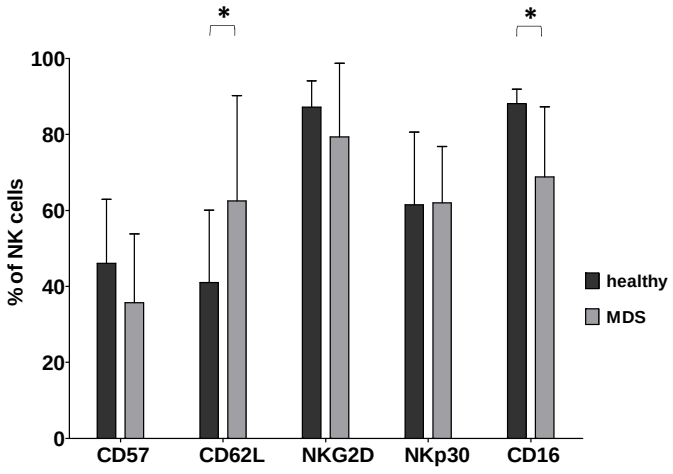

Figure S8

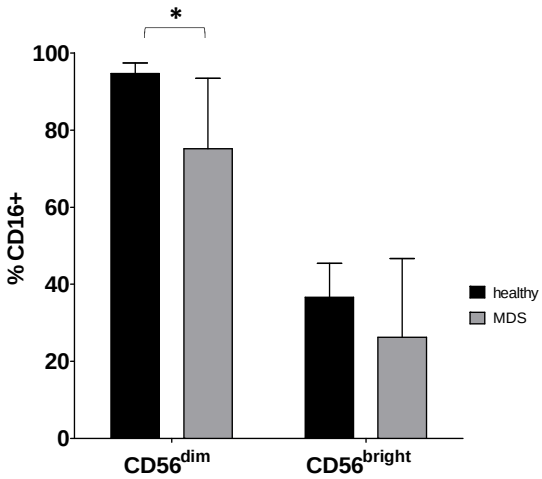

Figure S9